The Realtime Assessment of Mental Workload by Means of Multiple Bio-Signals

Master thesis Report

Methodology and Statistics for the Behavioral, Biomedical and Social Sciences

Utrecht University

Bart-Jan Boverhof, 6000142

Thesis Supervisor

Prof.dr.ir. B.P. Veldkamp

Date

January 11, 2020

1 Introduction

The topic of mental workload is a widely studied phenomenon across a variety of different fields, amongst others the field of ergonomics (Young, Brookhuis, Wickens, & Hancock, 2015), human factors (Pretorius & Cilliers, 2007) and neurosciences (Shuggi, Oh, Shewokis, & Gentili, 2017). A commonly utilized definition for mental workload, hereafter referred to as simply "workload", is the demand placed upon individuals whilst they carry out a particular task. As pointed out by De Waard and te Groningen (1996), the aforementioned definition is too simplistic, for it defines workload solely as an external phenomenon. Workload is, however, a person-specific construct, for the amount of perceived workload ushered by a given task may differ across individuals (De Waard & te Groningen, 1996). Hence, when referring to workload throughout this research, person-specific workload is implied specifically.

A commonly employed method for assessing workload is the well established NASA-Task Load Index questionnaire. This questionnaire inquires the respondent on the amount of perceived workload, and is constructed from six subjective sub-scales (Hart, 2006). Such an assessment is usually conducted post-experiment, which can in certain situations be deemed undesirable. Consider an experiment in which is aimed to assess workload of a pilot in flight. An evident approach towards such an experiment is that we wish to measure the degree of perceived workload during different phases of the flight. However, only after the simulation is concluded, a measurement in the form of a questionnaire can be administrated. In such a situation, utilizing a post-experiment assessment is prone to generate bias. A widely recognized bias is the observer-bias, advocating that participants in an experiment tend to overexaggerate the treatment effect when having to report it post-experiment (Mahtani, Spencer, Brassey, & Heneghan, 2018). In the light of the aforementioned example, pilots are expected to overexaggerate the degree of perceived workload when having to report it post-experiment.

An alternative approach to the assessment of workload is to collect physiological bio-signals during the experiment, and utilize these to classify workload. Examples of such bio-signals, hereafter referred to as "modalities", include techniques as electroencephalogram, eye-tracking, galvanic skin response, functional near-infrared spectroscopy etc. The advantage of such an approach is that complementary information streams, each stemming from a different modality, may all be interpreted simultaneously (Ramachandram

& Taylor, 2017). This has the potential of yielding a rich and multifaceted classification of construct such as workload. Additionally, it is possible to train a separate model for each individual, catering towards the individual perception of workload for that specific person. This approach, however, comes at the cost of an increase in complexity. This resides in the need to construct a complex framework that inputs the data from each of the utilized modalities, and ultimately outputs a single classification outcome.

The current research builds upon research conducted by Dolmans, Poel, van 't Klooster, and Veldkamp (in press), who proposed a deep-learning approach to multi-modular classification of workload. The current research differs from this previous endeavor in that it utilizes different modalities, and hence different data. In addition, the current research investigates upon the feasibility of a real-time approach. Real-time in this sense reflects the real-time classification of workload, i.e. the classification of workload whilst the experiment takes place. Doing so enables the possibility to conduct a dynamic experiment, the state of which can be altered by responding towards the classified degree of workload at a certain moment in time. Consider a simulation with the objective of educating its participant, such as a surgical simulation for educating surgeons-in-training. The learning experience of a single session could be dramatically enhanced when the state of the experiment is catered towards the individual learning process dynamically. For example, in case it is recognized early on in the simulation that a surgeon-in-training has difficulty with a specific procedure, the remainder of the experiment can be catered towards focusing on this specific procedure. By enhancing the learning experience in this way, the effectiveness of a single simulation session can be improved dramatically, entailing a more efficient learning process.

Three different modalities are utilized in the current research. Firstly the technique of electroencephalogram, hereafter referred to as "EEG", secondly the technique of galvanic skin response, hereafter referred to as "GSR" and thirdly the technique photoplethysmography, hereafter referred to as "PPG". It is of importance to recognize that the objective of the current research is not to gain insight into the most optimal model design for each of the previously delineated modalities. The objective is rather to construct a framework with which real-time classification can be managed, and to which modalities of choice can easily be added in future research endeavors. Consequently, one of two design principles on which the architecture of the framework reclines is the principle of modularity. Modularity refers to the extent to which different modalities can freely be added and/or removed to the framework, without the necessity to re-architect and rebuild it entirely. The second design principle is the principle of generalizability, prescribing that the framework should not merely be utilizable in the context of workload, but also for the measurement of other mental constructs.

A deep-learning approach towards the construction of a real-time multi-modular framework is realized. Considering the complexity and sheer size of such a deep-neural network, an important point of attention is classification speed. The challenge in real-time classification with deep-learning is often not reaching adequate performance, but rather to attain adequate speed of classification. Deep neural networks easily constitute thousands of calculations to be made simultaneously, which is even more true for a multi-modular approach such as the current. In order for real-time classification to work, classification cannot take too long, for otherwise it is not real-time anymore and the previously delineated benefit of a real-time approach dissipates. As a consequence, multiple networks are considered and contrasted in terms of performance and ability to classify in real-time. Firstly, for each of the three modalities separately, a single-modular network is constructed. Secondly, a multi-modular network is architected. Additionally, several variations to this multi-modular framework are considered and contrasted. These variations are specified to differ in size, i.e. the amount of neurons and filters.

The objective of the current research is to explore the circumstances in which a multi-modular approach by means of deep learning is capable of real-time classification, whilst still ensuring ample and adequate performance. Ultimately, this line of research pursues the ability to conduct a dynamic experiment for multiple people simultaneously, and of which the state can be altered in real-time.

2 Methods

2.1 Related Work

The current section will provide an overview of previous research on the most optimal network architecture for each modality separately. Additionally, the most feasible architecture for the multi-modular framework in its entirety will be explored. In particular, attention is placed upon the data fusion strategy, the real-time component and several model optimization techniques.

2.1.1 First modality: Electroencephalogram (EEG)

The first utilized modality is EEG, which constitutes a technique that detects electrical activity in the brain using electrodes. EEG is a widely utilized method for classifying workload. An overview of the complete literature on EEG classification with deep learning has been made by Craik, He, and Contreras-Vidal (2019), who reported a total of 16 % of all available papers to constitute with workload, lending credence to the ability of EEG as classifier of workload. Additionally, the usage of deep learning techniques for a range of different EEG application was investigated upon. Summarizing, it was reported that studies mostly found deep belief networks and convolutional neural networks to perform best when classifying workload, and advice one of these approaches as a consequence (Craik et al., 2019).

Research by Schirrmeister et al. (2017) contrasted the performance of several convolutional neural networks, hereafter referred to as "ConvNets", against the widely acknowledged baseline method for EEG classification, filter bank common spatial pattern, hereafter referred to as "FBCSP". The investigated networks included a deep, a shallow, a deep-shallow hybrid and a residual ConvNet. Both the deep and shallow ConvNets were found to reach at least similar, and in some regard better classification results, as compared with the FBCSP baseline. Altogether, a deep ConvNet with four convolutional-max-pooling blocks was found to perform best, displaying an accuracy of 92.4 % (Schirrmeister et al., 2017).

A different approach is proposed by Tabar and Halici (2016), combining a ConvNet with a Stacked auto-encoder network, hereafter referred to as "SAE". Within this network, the input layer feeds into a convolutional layer with the objective of learning the filters and network parameters. The output of this convolutional layer subsequently feeds into SAE part of the network, constituting an input layer, 6 hidden layers and an output layer. A classification accuracy of 90 % was acquired with this model (Tabar & Halici, 2016) .

2.1.2 Second modality: Galvanic Skin Response (GSR)

The second utilized modality is GSR, measuring sweat gland on the hands and hereby inferring arousal. GSR activity have been found to significantly increase as a consequence of an increase in task workload, hence constituting to be an objective predictor (Shi, Ruiz, Taib, Choi, & Chen, 2007).

Sun and colleagues explored the most optimal deep learning network for classifying six different emotional states by means of GSR data. Several models were investigated upon, amongst others a support vector machine, a ConvNet, a long-short-term-memory model and a hybrid model combining the ConvNet and long-short-term-memory, herefater referred to as "LSTM", approaches. The hybrid model was found to perform best, exhibiting an accuracy of 74% (Sun, Hong, Li, & Ren, 2019).

A variant on the CovNet LSTM model was employed by Dolmans et al. (in press), who aimed to classify workload by means of, amongst other modalities, also GSR. The performance of this model was contrasted with a network consisting solely of fully connected dense layers. Conform with findings by Sun et al. (2019), the hybrid model was found to perform best, displaying an accuracy of 82 % (Dolmans et al., in press). The model architecture as utilized by Dolmans et al. (in press) deployed two convolutional max-pooling blocks and two LSTM layers.

2.1.3 Third modality: Photoplethysmography (PPG)

The third modality constitutes PPG, which is a technique utilized to measure heart rate. PPG is, not undeservedly, a widely deployed technique within the field of workload classification. Zhang and colleagues investigated several approaches for measuring workload, comparing in total four modalities, out of which one was PPG. PPG was found to display both the highest sensitivity and reliability for measuring workload, lending credence to the feasibility of PPG as a method for classifying workload (Zhang et al., 2018).

Work by Biswas et al. (2019) investigated upon a deep learning approach towards PPG classification, with the objective to perform both bio-metric identification and obtain heart rate information. Exceptional results were attained with a neural network, attaining an average accuracy of 96 % (Biswas et al., 2019). This performance was managed with a hybrid model, incorporating two convolutional max-pooling blocks, followed with two LSTM layers.

2.1.4 Fusion strategy

When architecting a multi-modular network, information streams stemming from different modalities are required to be combined, i.e. "fused", at one point in the network in order to ultimately result in a single classification. Fusion can be done at different locations, and in different ways. Several fusion strategies as proposed by Ramachandram and Taylor (2017) have been considered.

Early, or data-level, fusion focuses on how to optimally combine data sources, before being fed into the network. Techniques that realize this include for example principle component analysis or factor analysis. Early fusing is usually challenging, especially for a multi-modular situation such as the current. This resides in the fact that data stemming from different modalities often differ with regards to dimensionality and sampling rate. Another disadvantage of early fusing, is that usually the oversimplified assumption of conditional independence is made. This assumption is unrealistic in practice, for data stemming from different modalities are expected to be correlated (Ramachandram & Taylor, 2017).

Late, or decision level, fusion on the other hand refers to the process of aggregating the decisions from multiple models, each separately applied on each modalitiy separately. In case the data sources stemming from the various modalities are either correlated or ultimately inhibit a different dimensionality, late fusion is a much more feasible approach (Ramachandram & Taylor, 2017).

Lastly, intermediate fusion is the most widely employed fusion strategy for multi-modal deep learning problems. Modalities are fused by concatenation and adding a higher order layer, to which the individual networks, separately defined for each modality, feed into. This need not be a single layer, but could be multiple layers, as long as each modality ultimately feeds into the highest order output layer. The depth of the fusion (i.e. the amount of fusion layers) can be chosen conform the specific situation, posing intermediate fusion to be the most flexible, and therefore the most widely utilized fusion strategy (Ramachandram & Taylor, 2017).

Indeed, when consulting the literature, intermediate fusion strategies are the most prevailing for multi-modular deep neural networks. When taking such an approach, one is required to consider the design of this higher order network. Rastgoo, Nakisa, Maire, Rakotonirainy, and Chandran (2019) utilize a multi-modular ConvNet approach, and fuse the modalities by concatenation, followed with two LTSM layers, two dense layers and a softmax layer. A simpler approach is utilized by Han, Kwak, Oh, and Lee (2020), who utilized an intermediate fusion approach solely consisting of several fully connected dense layers, and ending with a soft-max layer. Lastly, Dolmans et al. (in press) used a relatively deep intermediate fusion approach, consisting of two dense layers, two convolutional layers followed by another two dense layers.

2.1.5 Model optimization

The technique of batch normalization was proposed by Ioffe and Szegedy (2015), and is often applied in deep learning with the objective of enhancing the stability of a network. This is endeavored by including a batch normalization layer after each convolutional layer, re-centering and re-scaling the input feeding into this layer. If incorporating a batch normalization layer, it is recommended to do so before feeding into the activation function (Ioffe & Szegedy, 2015). An increase in accuracy for EEG classification was attained by Dolmans et al. (in press) and Schirrmeister et al. (2017) by specifying a batch normalization layer after each convolutional layer. Equally so, the best performing model for PPG data as proposed by Biswas et al. (2019) included a batch normalization layer after each convolutional layer.

Pooling layers are often used in ConvNets, following a convolutional layer with the attempt to decrease the dimensionality. The objective of such layers are to merge similar features into one (for a more extensive elaboration see: LeCun, Bengio, and Hinton (2015)). Considering the earlier delineated EEG ConvNets, both Schirrmeister et al. (2017) and Tabar and Halici (2016) specified a max-pooling layer after each convolutional layer. The network as proposed for GSR by Sun et al. (2019) incorporated a max-pooling layer after each, but one of the convolutional layers. Lastly, the network as proposed for PPG by (Biswas et al., 2019) specified a max pooling layer after each convolutional layer.

Hyper-parameter optimization, hereafter referred to as "HPO", is a technique that can be used to optimize hyper-parameter, such as for example learning rate, dropout probability and momentum. Substantial advancements within the deep learning community have been attained by utilizing HPO, especially considering the performance of ConvNets (Bergstra & Bengio, 2012). The Optuna toolbox provides a method for creating a parameter search space, from which values for the hyper-parameters can be sampled, and thus HPO can be performed (Akiba, Sano, Yanase, Ohta, & Koyama, 2019).

2.2 Data

The current section will provide an overview of the utilized data. Special attention is placed on the experimental setup, the description of the participants and the data collection / synchronization process.

2.2.1 Experimental setup

The experimental setting for data collection is the open-source spaceship video-game Empty Epsilon, in which the respondent is required to carry out tasks on a virtual spaceship (Daid & Nallath, 2016). This experiment is instituted by the Brain Computer Interfaces (BCI) testbed lab, hosted by the University of Twente and carried out in cooperation with Thales group Hengelo. The experiment constituted three different segments, during each of which the respondent had to carry out different tasks, all of which constructed to entail varying degrees of perceived workload. Each segment consists of six small sessions of roughly 5-10 minutes. These sessions varied in difficulty, including two easy, two intermediate and two hard sessions per segment. A schematic overview of the experimental structure is depicted as figure 1. After each of the 18 sessions, respondents filled in the TLX questionnaire consisting of 6 questions each, resulting in 18 filled in questionnaires. Each questionnaire inquired upon the degree to which the respondent experienced workload during the previous session. These ratings have been use as labels in later training of the network. Within each segment, the order in which the sessions (varying in difficulty) were presented have been randomized. The order in which the segments were administrated were not random. Between every three sessions, respondents were requested to take a short 2 minute break.

The first segment emulated a scenario in which hostile spaceships approach the respondent's spaceship. The respondent is required to quickly react by defusing hostile spaceships in order to survive. The increment in difficulty caused the process of defusing hostile spaceships to be more challenging, and hereby to take longer, aiming to increase workload as a consequence. The second segment emulated a scenario in which the respondent had to navigate their spaceship trough space, gathering as many way-points as possible. Obstacles around which the respondent had to carefully navigate were introduced in the intermediate difficult scenario, and hostile spaceships the respondent had to decimate were introduced in the hard scenario. Both increase difficulty, and hereby

Figure 1

Experimental setup

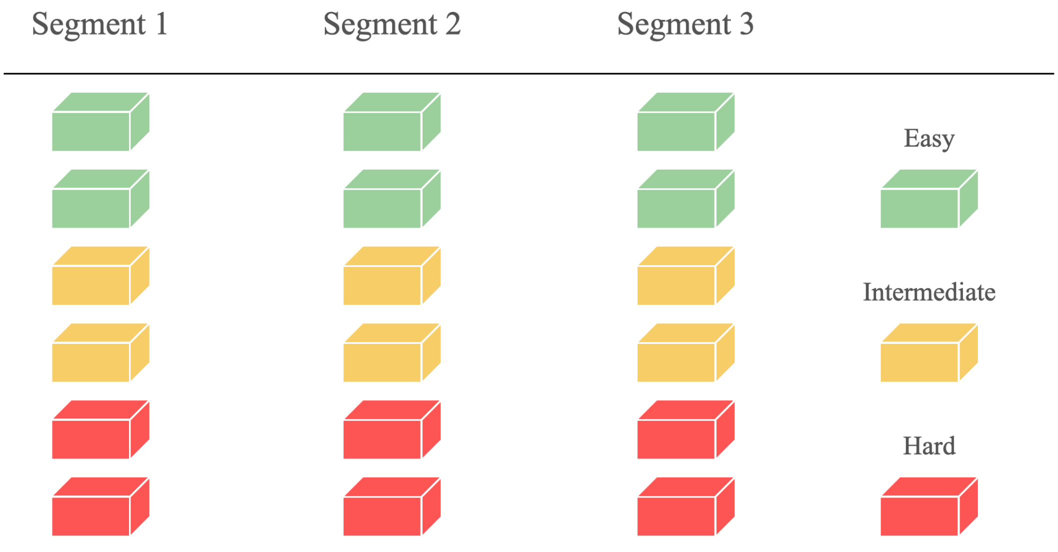

aim to increase workload as a consequence. The third and final segment emulated a machine room, in which respondents had to control the power based on randomly generated requests. Variables that could overheat the spaceship were introduced, demanding the respondent to multi-task, hence increasing difficulty.

2.2.2 Participants

In total, twenty-five respondents are participating in the study. Currently, the data is still in the process of being collected, for which no additional descriptive statistics can be presented in the this section as of yet. The respondents are students, recruited from the University of Twente. Recruitment has been conducted with Sona, which is a cloud-based participant management system. Requirements were that respondents didn't have any constraints that might interfere with the utilized sensors, such as for example a pacemaker. This was assessed by means of a short demographic questionnaire prior to the experiment. Additionally, the respondents were made aware of informed consent prior to the experiment, with the objective to ensure completely voluntary participation. Respondents were able to draw back from the experiment at any time.

2.2.3 Devices and Sampling Rate

The Shimmer3 GSR+ sensor was used for both PPG and GSR measurements. The device is worn on the wrist, and is able to communicate the signal wirelessly. An ear-clip was utilized for measuring PPG, and converting this to estimate heart rate. Skin conductivity, or GSR, was monitored by two electrodes attached to the fingers (Shimmer-Research, n.d.). EEG measurement is conducted with the Muse 2, which is a multi-sensor headband that provides feedback on brain activity (InteraXon, n.d.). The Shimmer3 GSR+ is able to read and output data signals on a sampling rate of 256 Hz, whereas the Muse 2 is able to sample at a maximum of 220 Hz.

As was already touched upon in the introduction, real-time classification requires a swift network. A higher sampling rate entails more data traveling through the network, decelerating classification speed. As a consequence, it is beneficial to input data on the minimum required sampling rate with which the key features can be detected for each modality in a consistent manner. Fujita and Suzuki (2019) investigated the minimum required sampling rate for the PPG modality. The extent to which features were detected have been contrasted for several sampling rates. A sampling rate of 60 Hz was found to be the absolute minimum required sampling rate for extracting all commonly utilized features stably (Fujita & Suzuki, 2019). A slightly higher sampling rate might be the safer option, however. Shimmer-Research (n.d.) recommend a sampling rate of 100 Hz for the PPG modality, and stable feature extraction was naturally observed on this rate by Fujita and Suzuki (2019) as well. Hence, a sampling rate of 100 Hz is utilized for the PPG modality. The required sampling rate for the GSR modality is substantially lower as compared with both PPG and EEG. Shimmer recommended the necessary sampling rate to range between 0.03 and 5 Hz (Shimmer-Research, n.d.). A sampling rate of 5 Hz will be utilized consequently. For the EEG modality, different features require a widely different sampling rate in order to be detected. Frequency bands for traditional EEG features are defined on about 0.5-4 Hz for delta, and at most on about 16-24 Hz for beta. The gamma frequency band recently gained in popularity within the field of EEG, and is defined on a frequency ranging up to 80 Hz (Weiergraeber, Papazoglou, Broich, & Mueller, 2016). In order to detect a feature residing on the 80 Hz frequency band, a substantially higher sampling rate is required to record the signal without aliasing. The required sampling rate can be determined by means of the Nyquist criterion for practical EEG sampling, defined as equation 1,

$$f_{samp} > 2.5 * f_{max} \tag{1}$$

where f_{sam} reflects the required sampling rate and f_{max} reflects the frequency range around which the feature to be detected resides(Srinivasan, Tucker, & Murias, 1998). Hence, in order to be able to detect the gamma frequency band, a sampling rate of 200 is utilized for the EEG modality. A summary of the utilized sampling rates per modality is depicted as table 1.

Table 1

Sampling rate per modality

	Utilized sampling rate (Hz)
Electroencephalogram (EEG)	200
Galvanic Skin Response (GSR)	5
Photoplethysmography (PPG)	100

2.2.4 Synchronization

Data streams stemming from the different modalities were required to be properly synchronized such that they are parallel. This was accomplished by means of an application called Lab-Streaming Layer, hereafter refered to as "LSL", to which the different data are streamed during the experiment. LSL properly synchronized these data streams, such that they refer to the same points in time, and subsequently record all data into a single file per participant (Kothe, Medine, & Grivich, 2018).

2.3 Framework Architecture

As was elaborated on in the introduction, several networks will be compared in their ability to classify workload in real-time, and the performance with which this is managed. The upcoming section opens with the description of the network architectures solely utilizing one of the three modalities each. Subsequently, the multi-modular architecture will be elaborated on. Lastly, several variations based on this multi-modular architecture are delineated.

Figure 2

Three single-modular network architectures

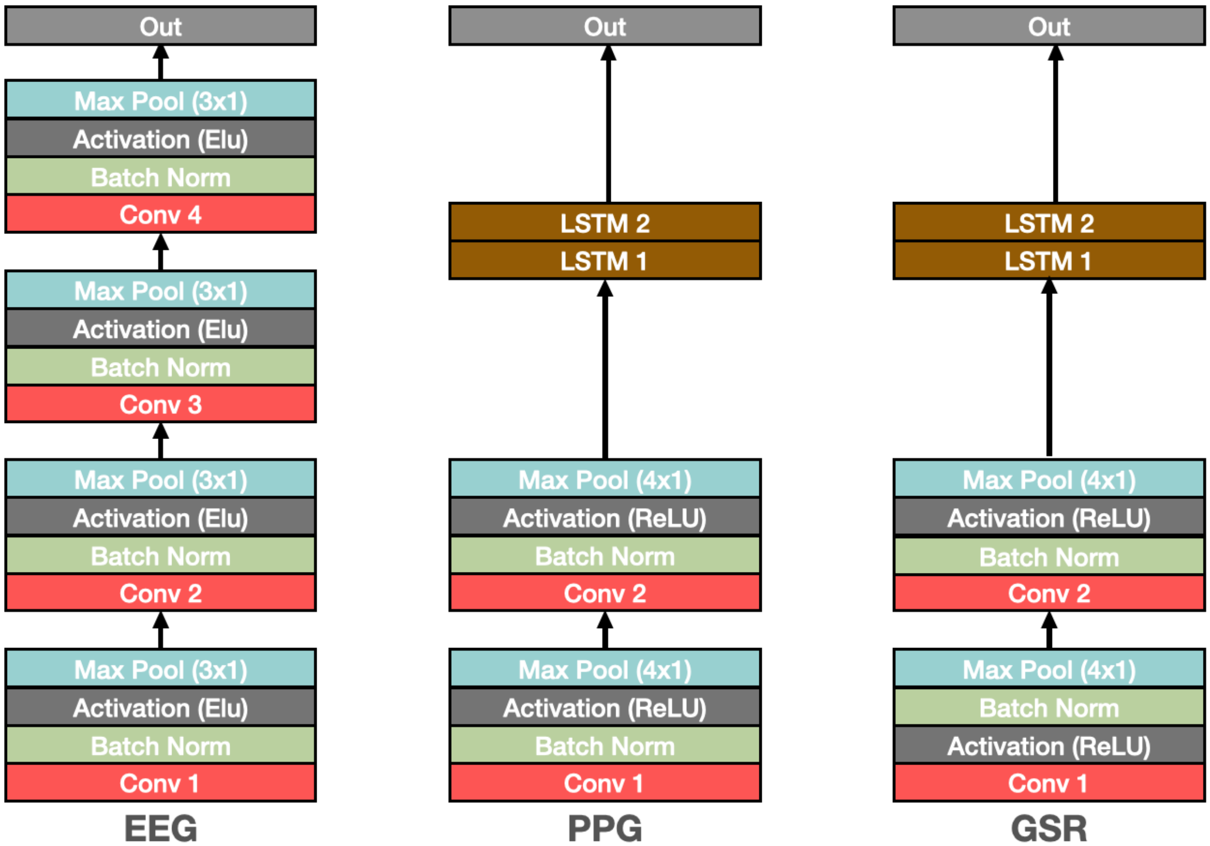

2.3.1 Single-modular Network Architectures

The architecture of each of the single-modular networks is determined by combining insights from the literature. Each of the three network merely utilizes a single modality with which workload is classified. These networks and their architecture are all depicted as figure 2.

The utilized network for the EEG modality is a ConvNet, as proposed by Schirrmeister et al. (2017). The network is designed to include four convolutional blocks, each constituting a convolutional layer, followed by a batch normalisation layer. The Exponential Linear Unit, hereafter referred to as ”ELU”, function is utilized as activation function, and is defined as equation 2. Each convolutional block is closed with a max pooling layer of stride three.

$$f(x) = \begin{Bmatrix} x & x \geq 0 \\ \alpha(e^x - 1) & x < 0 \end{Bmatrix} \tag{2}$$

The utilized network for the GSR modality is a LSTM ConvNet network, inspired by the work of Sun et al. (2019) and Dolmans et al. (in press). The network is designed to include two convolutional blocks, each constituting a convolutional layer, followed by a batch normalization layer, an activation layer and closed with a max-pooling layer of stride four. The Rectified Linear Unit, hereafter referred to as "ReLU", function is utilized as activation function, defined as equation 3. Following these two convolutional blocks are two LTSM layers.

$$f(x) = max(0, x) \tag{3}$$

Lastly, the utilized network for the PPG modality is inspired upon the network as proposed by Biswas et al. (2019). The nework opens with two convolutional blocks, each consisting of a convolutional layer, batch normalization layer, activation layer and closed with a max pooling layer of stride four. The utilized activation function is the ReLU, depicted as equation 3. Following these convolutional blocks are two LTSM layers, equal to the GSR model.

2.3.2 Multi-modular Network: Architecture

The network architecture that is utilized for the multi-modular approach is determined by a combination of the single-modular networks, as derived from the literature. The previously delineated design principles (i.e. the principles of modularity and generalizability) are taken into account when doing so. A visual representation of the multi-modular network is depicted as figure 3.

In order to combine the previously delineated single-modular networks, each of these distinct parts are closed with one fully connected dense layer before feeding into the head network. This is done in order to flatten all inputs into a lower dimensional space, such that concatenation is possible. The head network consists of four dense layers. These layers are alternated with a batch normalization and max-pooling layer with the objective

Figure 3

Multi-modular Network Architecture

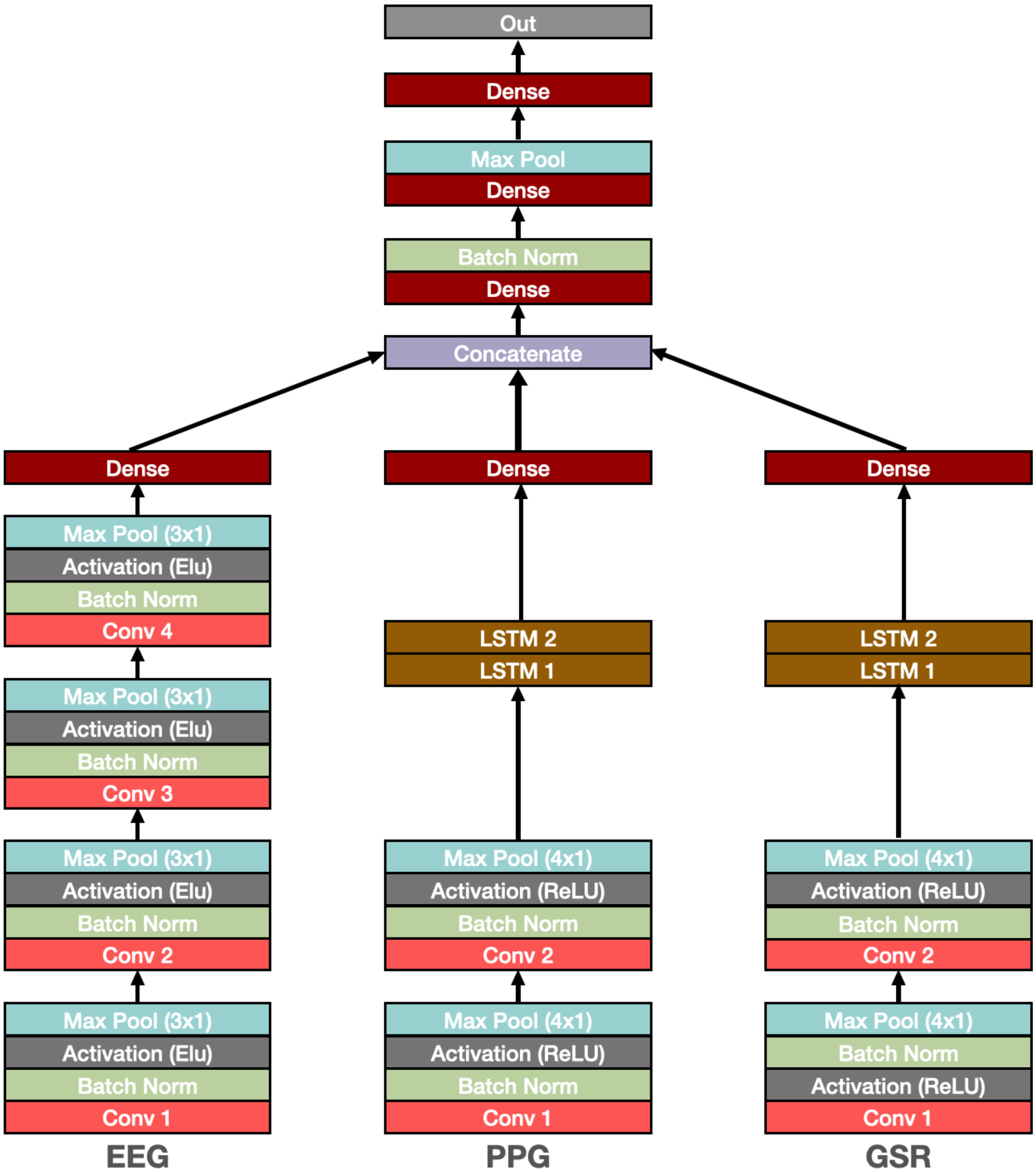

of stabilization.

2.3.3 Multi-modular Network: Variations

Multi-modular classification in real-time by means of deep-learning requires an optimized network, as was elaborated upon in the introduction. Speed is a potential bottleneck, for a multi-modular network such as presented is substantially complex in nature. Therefore, several variations of the delineated network will be investigated upon, differing in their complexity. These variations are not made by changing the network architecture, whereas deviating from the proven network architecure is likely to be detrimental with regards to model performance. The aim is to propose a network that is fast enough for real-time classification, whilst maintaining the highest amount of accuracy as possible. Three different variations with regards to size of the network as depicted in figure 3 will therefore be considered.

Network size is understood as the amount of utilized filters for convolutional layers, and the amount of neurons for all other utilized layers. A decrease in the amount of filters and neurons constitutes a decrease in network size, and consequently a decrease in the amount of required calculations. This is likely to bring about an increase in speed. An overview of all three multi-modular network variations, and the amount of utilized neurons/filters is provided in table 2. Network 1 is referred to as the full network, and is the biggest in terms of size. The size of network 2 constitutes of 75 % of the size of the full network. Network 3 constitutes of 50 % of the size of the full network.

Table 2

Model variation sizes

	EEG	GSR	PPG	Head
Network 1	Conv1: 25	Conv1: 128	Conv1: 128	Dense: 712
	Conv2: 50	Conv2: 128	Conv2: 128	Dense: 356
	Conv3: 100	LSTM1: 256	LSTM1: 256	Dense: 178
	Conv4: 200	LSTM1: 256	LSTM2: 256	
	Dense: 200	Dense: 256	Dense: 256	
Network 2	Conv1: 18	Conv1: 96	Conv1: 96	Dense: 534
	Conv2: 34	Conv2: 96	Conv2: 96	Dense: 267
	Conv3: 75	LSTM1: 192	LSTM1: 192	Dense: 134
	Conv4: 150	LSTM1: 192	LSTM1: 192	
	Dense: 150	Dense: 192	Dense: 192	
Network 3	Conv1: 13	Conv1: 64	Conv1: 64	Dense: 356
	Conv2: 25	Conv2: 64	Conv2: 64	Dense: 178
	Conv3: 50	LSTM1: 128	LSTM1: 128	Dense: 89
	Conv4: 100	LSTM1: 128	LSTM2: 128	
	Dense: 100	Dense: 128	Dense: 128	

Note: For all convolutional layers the depicted number reflects the amount of utilized filters, whereas for LTSM layers it reflects the amount of nodes.

2.4 Model Evaluation

The performance of the four network variations will be contrasted by means of several performance metrics. The utilized metrics constitute six well known and widely applied metrics, all constructed from the confusion matrix, depicted as table 3.

Table 3

Confusion matrix

	True Positive	True Negative
Predicted Positive	a	b
Predicted Negative	c	d

The measures accuracy, sensitivity, specificity, PPV, NPV and F1 will be utilized in order to asses network performance. The network that performs best across these measures is considered to be the superior performing network. Table 4 depicts the constitution of these performance metrics, by partly referring to confusion matrix depicted as table 3.

Table 4

Performance Metrics

Accuracy:	$\frac{a+d}{a+b+c+d}$
Sensitivity:	$\frac{a}{a+c}$
Specificity:	$\frac{d}{b+d}$
Positive Predicted Value (PPV):	$\frac{a}{a+b}$
Negative Predicted Value:	$\frac{d}{c+d}$
F1-measure:	$\frac{2*Sensitivity*PPV}{Sensitivity+PPV}$

References

Akiba, T., Sano, S., Yanase, T., Ohta, T., & Koyama, M. (2019). Optuna: A next-generation hyperparameter optimization framework. In *Proceedings of the 25th acm sigkdd international conference on knowledge discovery & data mining* (pp. 2623–2631).

Bergstra, J., & Bengio, Y. (2012). Random search for hyper-parameter optimization. *The Journal of Machine Learning Research*, *13*(1), 281–305.

Biswas, D., Everson, L., Liu, M., Panwar, M., Verhoef, B.-E., Patki, S., ... others (2019). Cornet: Deep learning framework for ppg-based heart rate estimation and biometric identification in ambulant environment. *IEEE transactions on biomedical circuits and systems*, *13*(2), 282–291.

Craik, A., He, Y., & Contreras-Vidal, J. L. (2019). Deep learning for electroencephalogram (eeg) classification tasks: a review. *Journal of neural engineering*, *16*(3), 031001.

Daid, & Nallath. (2016). *Empty epsilon multiplayer spaceship bridge simulation.* URL: https://github.com/daid/EmptyEpsilon. GitHub.

De Waard, D., & te Groningen, R. (1996). *The measurement of drivers' mental workload.* Groningen University, Traffic Research Center Netherlands.

Dolmans, T., Poel, M., van 't Klooster, J.-W., & Veldkamp, B. (in press). Percieved mental workload detection using intermediate fusion multi-modal networks.

Fujita, D., & Suzuki, A. (2019). Evaluation of the possible use of ppg waveform features measured at low sampling rate. *IEEE Access*, *7*, 58361–58367.

Han, S.-Y., Kwak, N.-S., Oh, T., & Lee, S.-W. (2020). Classification of pilots' mental states using a multimodal deep learning network. *Biocybernetics and Biomedical Engineering*, *40*(1), 324–336.

Hart, S. G. (2006). Nasa-task load index (nasa-tlx); 20 years later. In *Proceedings of the human factors and ergonomics society annual meeting* (Vol. 50, pp. 904–908).

InteraXon. (n.d.). *Muse 2 brainwave activity headband.* Retrieved from `https://choosemuse.com/muse-2/`

Ioffe, S., & Szegedy, C. (2015). Batch normalization: Accelerating deep network training by reducing internal covariate shift. *arXiv preprint arXiv:1502.03167*.

Kothe, C., Medine, D., & Grivich, M. (2018). Lab streaming layer (2014). *URL: https://github. com/sccn/labstreaminglayer (visited on 02/01/2019)*.

LeCun, Y., Bengio, Y., & Hinton, G. (2015). Deep learning. *nature*, *521*(7553), 436–444.

Mahtani, K., Spencer, E. A., Brassey, J., & Heneghan, C. (2018). Catalogue of bias: observer bias. *BMJ Evidence-Based Medicine*, *23*(1), 23.

Pretorius, A., & Cilliers, P. (2007). Development of a mental workload index: A systems approach. *Ergonomics*, *50*(9), 1503–1515.

Ramachandram, D., & Taylor, G. W. (2017). Deep multimodal learning: A survey on recent advances and trends. *IEEE Signal Processing Magazine*, *34*(6), 96–108.

Rastgoo, M. N., Nakisa, B., Maire, F., Rakotonirainy, A., & Chandran, V. (2019). Automatic driver stress level classification using multimodal deep learning. *Expert Systems with Applications*, *138*, 112793.

Schirrmeister, R. T., Springenberg, J. T., Fiederer, L. D. J., Glasstetter, M., Eggensperger, K., Tangermann, M., ... Ball, T. (2017). Deep learning with convolutional neural networks for eeg decoding and visualization. *Human brain mapping*, *38*(11), 5391–5420.

Shi, Y., Ruiz, N., Taib, R., Choi, E., & Chen, F. (2007). Galvanic skin response (gsr) as an index of cognitive load. In *Chi'07 extended abstracts on human factors in computing systems* (pp. 2651–2656).

Shimmer-Research. (n.d.). *Shimmer3 gsr unit.* Retrieved from `https://www.shimmersensing.com/products/shimmer3-wireless-gsr-sensor`

Shuggi, I. M., Oh, H., Shewokis, P. A., & Gentili, R. J. (2017). Mental workload and motor performance dynamics during practice of reaching movements under various levels of task difficulty. *Neuroscience*, *360*, 166–179.

Srinivasan, R., Tucker, D. M., & Murias, M. (1998). Estimating the spatial nyquist of the human eeg. *Behavior Research Methods, Instruments, & Computers*, *30*(1), 8–19.

Sun, X., Hong, T., Li, C., & Ren, F. (2019). Hybrid spatiotemporal models for sentiment classification via galvanic skin response. *Neurocomputing*, *358*, 385–400.

Tabar, Y. R., & Halici, U. (2016). A novel deep learning approach for classification of eeg motor imagery signals. *Journal of neural engineering*, *14*(1), 016003.

Weiergraeber, M., Papazoglou, A., Broich, K., & Mueller, R. (2016). Sampling rate, signal bandwidth and related pitfalls in eeg analysis. *Journal of neuroscience methods*, *268*, 53–55.

Young, M. S., Brookhuis, K. A., Wickens, C. D., & Hancock, P. A. (2015). State of science: mental workload in ergonomics. *Ergonomics*, *58*(1), 1–17.

Zhang, X., Lyu, Y., Hu, X., Hu, Z., Shi, Y., & Yin, H. (2018). Evaluating photoplethysmogram as a real-time cognitive load assessment during game playing. *International Journal of Human–Computer Interaction*, *34*(8), 695–706.